Progress in Organic Coatings 77 (2014) 1264–1270

Contents lists available at ScienceDirect

Progress in Organic Coatings

journal homepage: www.elsevier.com/locate/porgcoat

An electrochemical and mechanical approach to the corrosion resistance of cathodic electrocoatings under combined cyclic and DC polarization conditions

Sepehr Lajevardi Esfahani[a], Zahra Ranjbar[a,b,*], Saeed Rastegar[c]

[a] Faculty of Surface Coatings and Novel Technologies, Institute for Color Science and Technology, Tehran, Iran
[b] Center of Excellence for Color Science and Technology, Tehran, Iran
[c] Amirkabir University of Technology, Faculty of Polymer and Color Engineering, Tehran, Iran

ARTICLE INFO

Article history:
Received 6 August 2013
Received in revised form 13 February 2014
Accepted 29 March 2014

Keywords:
Cyclic test
EIS
Polarization
Electrocoated films
Corrosion

ABSTRACT

A modified AC/DC/AC test has been introduced. It consists of a combination of EIS test, cathodic polarizations, wet and dry cycles. This test method was applied to cathodically electrocoated mild steel substrates baked at different conditions. This study aims at characterizing protective behavior of under-, normal- and over-baked electrocoatings under cyclic corrosion conditions. It was found that the resistive failure is the dominant failure mechanism of all the coatings in this test. It was also found that a low crosslink density coating withstands the mechanical stresses due to dry–wet cycles better than a higher crosslink density one.

1. Introduction

The automotive industry requires organic protective coatings with high resistance to degradation. Protective properties of an organic coating must be tested in fairly short times. Protection against corrosion in automobiles is of great importance from the viewpoint of the national economy and the private car owner. Today, it can be stated that corrosion protection of almost all automobile bodywork includes a cataphoretic primer [1–4].

Corrosion test methods for painted metals can be divided nearly into two groups; electrochemical and non-electrochemical tests. Electrochemical tests can be run by either DC or AC power supplies [5].

Electrochemical impedance spectroscopy (EIS) is used widely to investigate the behavior of coated metals immersed in aggressive solutions. Determining the electrochemical impedance over a large frequency range (100 kHz-several mHz) provides information about various processes involved in protective behavior of the coatings. EIS is a useful technique in the study of corrosion performance of protective primers. Performing this test on a coated metal may take days, weeks and sometimes months before getting to good results [6–10].

So far, many studies have used electrochemical techniques such as EIS, to evaluate the performance of protective properties of different materials. The EIS test method provides quantitative information about the mechanism of corrosion process and protective properties of coatings such as pore resistance (R_{po}) and coating capacitance (C_c). In this method, the electrical parts of the equivalent circuit are related to decline rate of the protective properties of organic coatings under corrosive conditions [11–13].

Song and Liu [14] investigated the effect of substrate pretreatment on the corrosion resistance of electroless-coated AZ31 alloy using immersion, salt spray, cyclic exposure, EIS, XPS and XRD tests. The results showed that the coating protection performance can be significantly improved if the substrate surface is properly dehydrated at a high temperature after wet cleaning.

Zhou et al. [15] used an EIS accelerated test method to predict service lifetime of corrosion protective coatings. They used flowing deionized water to accelerate coatings degradation and reported that the EIS modulus decreased more in deionized water than in electrolyte solutions.

Bi and Sykes [16] investigated cathodic disbonding of an un-pigmented epoxy coating on mild steel under semi- and full-immersion in a 3.5 wt.% NaCl solution. Disbonding and growth of blisters were monitored by scanning acoustic microscopy, which showed growth of blisters within the disbonded area.

* Corresponding author at: Faculty of Surface Coatings and Novel Technologies, Institute for Color Science and Technology, Tehran, Iran. Tel.: +98 021 229 44 184/021 229 58319; fax: +98 021 229 58319.
E-mail addresses: ranjbar@icrc.ac.ir, roshanakranjbar@yahoo.com (Z. Ranjbar).

http://dx.doi.org/10.1016/j.porgcoat.2014.03.028
0300-9440/

The results of Wang et al. [17] showed that Mg-rich primers could be an adequate alternative for chromate-based coatings for protecting aluminum alloy from corrosion. In their research, EIS and noise measurements were conducted to monitor the electrochemical properties of the system beneath the topcoat.

Macedo et al. [18] characterized three different coatings (epoxy, alkyd, polyurethane paints) by electrochemical impedance measurements; permeability tests, free-standing film impedance and local impedance measurements. The results manifest that electrochemical impedance methods (global and local) are excellent tools to monitor the behavior of organic coatings. However these techniques alone are not enough to screen different paints.

There is an explicit interest in rapid assessment methods for practical applications, which provide a faster indication of corrosion processes in the coated metals. Hollaender et al. [19–21] for the first time in 1970 developed a rapid method for evaluating protective properties of coated metals used in food packaging. This combined method (AC/DC/AC test) consisted of applying a direct current (DC) and an electrochemical method based on altering current (AC). Suay et al. [2,3,22–24] used the electrochemical AC/DC/AC test to investigate the protective behavior of powder coatings and electrocoatings applied to steel substrates. Bierwagen and colleagues [25,26] electrochemically evaluated the in situ corrosion at metal/coating interface using accelerated AC/DC/AC test and embedded electrodes. Allahar et al. [27,29] characterized the potential changes at relaxation step of modified AC/DC/AC test (the AC/DC/AC test coupled with wet and dry cycles) by a mathematical model for calculating the characteristic times.

The AC/DC/AC test uses EIS to observe the condition of the coating before and after applying the DC potential.

The test consists of three steps:

The coated panel is immersed in the test solution until a stable OCP (open circuit potential) is observed. Then

(1) An EIS measurement is run to find out the initial condition of the coating;
(2) A DC potential is applied to generate an alkaline environment and stimulate delamination; and
(3) An EIS measurement is run to assess the condition of the coating after cathodic polarization.

Steps 2 and 3 are repeated to apply more stresses until the anti-corrosion properties of the sample are lost.

Any change in the impedance spectrum can be attributed to a coating deterioration (pore formation) and a delamination process at the metal–coating interface due to hydrogen gas and hydroxyl ion generation (if a cathodic reaction takes place) or induced mechanical stresses in dry/wet cycles [23–26].

The modified AC/DC/AC test consists of a DC potential application (cathodic polarization) together with soaking and drying cycles [27]. Soaking cycle is considered for stabilization of the sample in the saline solution before applying the DC potential. The dry cycle is considered for stress relaxation of samples and development of mechanical stresses if corrosion products are formed in pores of the coating film.

The DC potential application step is considered for acceleration of coating degradation through these three ways:

(1) Loss of adhesion of the coating to the substrate because of the hydrolysis reaction of absorbed water and formation of hydrogen gas.
(2) Coating degradation at metal/coating interface due to hydroxyl ion formation and a rise in pH.
(3) Dissolution of oxide or conversion coating layer and formation of a layer at coating/substrate interface which is a very strong conductor of electrons [20,21,27].

On the other hand, the cathodic delamination process is influenced by heterogeneous reactions at the metal–coating interface, homogeneous reactions, and transport of species within the partially disbonded coating section [27,28].

Organic coatings used in outdoor environment are constantly exposed to soaking and drying conditions. Mechanism of the corrosion process in outdoor conditions differs from the mechanism of corrosion in bulk of solution. Cyclic soaking and dry steps cause expansion and contraction of the coating film and develop more mechanical stresses in the coating film [30–35].

These cyclic stresses lead to chemical and mechanical changes, and finally degradation of the coating [36,37].

Parke et al. [38] monitored the absorption of water in a two-coat coating system, comprising an epoxy and a urethane layer, under a cyclic wet–dry condition using AC impedance method. The coated specimens were exposed to the alternate conditions of 4 h immersion in a 0.5 M NaCl solution and 8 h drying at 25 °C and 60% RH. The mechanism of corrosion beneath organic coatings under cyclic wet–dry exposure in chloride containing environments was discussed based on water uptake.

Cruz and Tsuru [39] evaluated the corrosion of stainless steel under a wet–dry cyclic condition using the AC impedance technique. Three types of stainless steel were exposed to the alternate conditions of 1 h immersion in a chloride containing solution and 5 h drying at 25 °C and 60%RH. The results showed that corrosion rate monitoring using an AC impedance method was possible under the given exposure conditions, even during the drying period as long as the metal was covered with a thin electrolyte layer.

Allahar and colleagues [27] evaluated the protective properties of an epoxy coating with average thickness of 88 microns, which was applied by spraying on normal steel using modified AC/DC/AC test.

In this research we used a modified AC/DC/AC procedure coupled with dry and wet cycles to investigate the effect of baking condition on protective properties of an automotive cathodic electrocoating primer.

2. Experimental

2.1. Materials

A commercial protective cathodic electrocoating material (CathoGard 500 supplied by BASF Company) was electrocoated on tri cationic phosphated mild steel substrates. Coatings were deposited for two minutes at a deposition voltage of 280 V to get 20 μm thick films. Stainless steel anodes were placed parallel to the steel panels (20 cm × 10 cm × 0.2 cm) at a distance of 19.0 cm. The temperature of the electrophoretic bath was kept between 28 and 30 °C. The anode: cathode area ratio was 1:3. The deposited films were baked at three different conditions corresponding to under-, normal- and over-baking of the electrocoating. Sample identifications and curing conditions are summarized in Table 1.

Table 1
Identifications and specifications of samples (application voltage: 280 V, application time: 120 s).

Sample identification	Curing temperature (°C)	Curing time (min)	T_g (°C)
U	145 ± 2	15	59
N	165 ± 2	20	90
O	190 ± 2	20	228

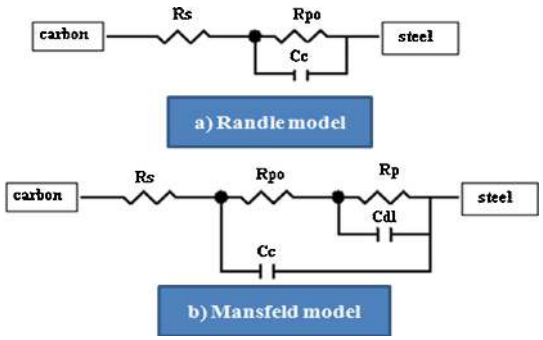

Fig. 1. Equivalent circuit models used for fitting EIS data.

2.2. Testing methods and equipment

The experiments were designed to confirm the reproducibility of the tests. All tests were repeated three times for each sample and the total number of experiments was 30.

2.2.1. Differential scanning calorimetry (DSC)

A Perkin Elmer DSC7 differential scanning calorimeter was used for dynamic scans to measure the glass transition temperature (T_g) of electrocoatings cured at different conditions. The average weight of samples was 6 mg and DSC scans were performed on samples at 10 °C min^{-1} to determine the midpoint T_g.

2.2.2. Electrochemical impedance spectroscopy (EIS)

First, the surface of electrocoated samples, except for the sample U, was cleaned by isopropylalcohol. Then an area of 1 cm^2 from the surface of each electrocoated samples was selected and the rest of the sample was fully covered with beeswax/rosin mixture. EIS tests were carried out on coated samples exposed to a 3.5% (w/w) NaCl solution in deionised water. A three-electrode electrochemical cell was set up. The exposed surface area was 1.00 cm^2. A graphite rod was used as the counter electrode and an Ag/AgCl electrode was used as the reference electrode with KCl concentration of 3.5 M. The impedance tests were carried out over a frequency range of 100 kHz down to 1 mHz using a sinusoidal perturbation voltage of 10 mV from peak to peak. The whole setup was placed inside a Faraday cage to reduce external interferences on the system. EIS tests were carried out under open-circuit conditions. The impedance spectrum was analyzed using the Z-view software.

The equivalent circuit models, shown in Fig. 1, were employed to analyze the EIS spectra. Here R_s is the electrolyte resistance, R_{po} and C_c are the pore resistance and film capacitance, respectively, and R_p and C_{dl} correspond to polarization resistance and double layer capacitance at the coating–metal interface. By fitting the equivalent circuit to the EIS data, values of the equivalent circuit elements were determined. The chi-squared limit of the fit was mostly below 0.1. In addition, the impedance parameters were normalized to the surface area of the samples.

2.2.3. Modified AC/DC/AC test

The modified AC/DC/AC procedure consists of a combination of water soaking (wet) step, dry step, DC potential application and AC measurement. At first an AC impedance spectrum was acquired from the sample immersed in the electrolyte for a certain time. This measurement allows the first state of the test sample to be determined. Following the first AC measurement, the test sample was immersed in a 3.5% (w/w) NaCl solution for 24 h as the wet step. Then the test sample was exposed to a constant cathodic voltage (−4 V) for 20 min and was subsequently placed in a desiccator for 24 h to dry completely. The sample was allowed to relax afterwards and a new equilibrium state was reached. This was shown by a stable OCP. In this case the relaxation time was 1–3 h. During that time, the variation of the system's potential as a function of time was recorded (relaxation time). Final EIS spectrum was collected to determine the new equilibrium state of the film. A schematic representation of the modified AC/DC/AC procedure is shown in Fig. 2.

Table 2
Definition of the signs used in Fig. 2.

	EIS test in 3.5% (w/w) NaCl in deionised water
	Soaking step for 24 h
	DC polarization (−4 V @20 min)
	Dry step for 24 h
	Relaxation step for 3 h

Table 2 shows definition of the signs used in Fig. 2. This test sequence was repeated 6 times for all the samples.

2.2.4. Gravimetric test

The surface of electrocoated samples, except for sample U, was cleaned by isopropyl alcohol.

Then an area of 1 cm^2 from the surface of each electrocoated sample was selected and the rest of the sample was fully covered with beeswax/rosin mixture. The initial weight of each sample was measured with an accuracy of 0.1 mg before immersing them into a solution of 3.5% (w/w) NaCl in deionized water for 7 days (soaking step). Then the samples were weighed again and afterwards were placed in a desiccator for 24 h (dry step). After the dry step, the weight of the samples was measured again. This process lasted for 20 days. The time program of the gravimetric test during the soaking and dry steps is shown schematically in Fig. 3.

2.2.5. Optical microscopic examination

Optical microscopic examination was carried out on the samples using the light microscope (Dual scope DS 95-200E) after the modified AC/DC/AC test.

3. Results and discussion

3.1. DSC test

The glass transition temperature (T_g) of the electrocoated samples, obtained from DSC tests, are listed in Table 1.

According to the DSC results, T_g of the sample (U) is less than that of the other samples because of its incomplete curing and lower final cross-linking density. The network of the binder in this sample should have a high free volume content. There is only a slight difference between the T_g value of sample (U) and room temperature (23 ± 2 °C), so the sample (U) is expected to be more flexible than the other samples. The DSC results of the samples (O) and (N) imply that the final cross-linking density of these samples is high enough. Therefore samples (N) and (O) are expected to be harder and less flexible.

3.2. Modified AC/DC/AC test

Bode plot representation of EIS spectrum of the electrocoated samples in modified AC/DC/AC test is shown in Figs. 4–6.

Fig. 7 shows the stable open circuit potentials of the electrocoated samples after 1 h of relaxation against the number of AC/DC/AC cycles.

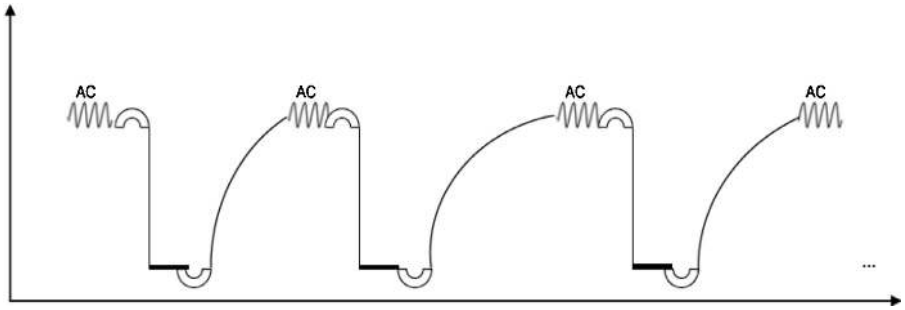

Fig. 2. Schematic representation of modified AC/DC/AC procedure.

The variation of pore resistance and coating capacitance of different samples as a function of the number of exposure cycles are shown in Figs. 8 and 9, respectively.

3.2.1. Electrochemical and Molecular Explanation

Fig. 7 indicates that the initial stable OCP value of all the samples has a larger value compared to the stable OCP values after any DC cycle application. This can be attributed to the fact that before DC application the osmotic-pressure is the dominant factor for penetrating hydrated ions of the electrolyte into the coating film, whereas the diffusion of the ions into a coating which is going through a large DC field (in this case 2×10^5 V m^{-1}) is mostly controlled by the electro-osmosis phenomena. As cycles of DC application rises, more counter ions diffuse into the coating and eventually accumulation of the counter ions at the coating–metal interface is expected. On the other hand, having a look at the variations of the pore resistance of the coatings (Fig. 8) suggest that a critical cycle number can be found after which the resistive mesh of the polymeric binder gets looser and the pore resistance drops 2–5 orders of magnitude, depending on the baking conditions. This critical DC cycle number is 2 for the normal- and over-baked samples, and 3 for the under-baked sample. We will come back to this point later in this paper.

Fig. 7 implies that the normal- and over-baked samples show a positive stable OCP value compared to a negative value for the under-baked sample. This may be a result of the more compact structure of the normal- and over-baked coatings. In a coating with a loosely cross-linked structure and an almost open resistive mesh the final stable OCP value is more negative and closer to equilibrium potential of oxidation of iron in the test electrolyte. As mentioned above, the under-baked coating with its loose polymeric network shows a lower initial pore resistance compared to the normal- and over-baked samples. This can also provide evidence that the initial structure of the over- and normal-baked coatings is more compact compared to that of the under-baked coating. Therefore a more durable protective behavior is expected for the over- and normal-baked samples. If this is true, why the stable OCP value for the normal- and over-baked coatings drop after 2 DC cycles whereas this drop is observed for the under-baked sample after 3 DC cycles? The key point in explaining this observation is the different behavior of the under-baked coating against the wet and dry cycles due to its different mechanical properties. Before explaining the mechanical concepts behind the observed trend for pore resistance and stable OCP values, let us look at Figs. 6 and 7 again. After the critical DC cycle, the pore resistance and the stable OCP values of the samples rise and nearly recover their initial value and then drop again to their final values. After the critical DC cycle the resistive structure of the coating may so open that the corrosion products could be formed and be piled-up at the coating–metal interface. These fragile materials are then removed from the interface during the later cycles and the interface is exposed to the electrolyte solution again. This results in a drop in both the pore resistance and the stable OCP values of all the samples.

Fig. 9 shows the variation of the coating capacitance for different coatings as a function of cycle number. The value of the coating capacitance is almost constant during the cyclic tests. This can indicate that the failure of the coatings during the DC test is mostly caused by the failure of their resistive elements.

Results of the gravimetric test during soaking and dry cycles are shown in Fig. 10. As specified in Fig. 10, all the electrocoatings absorbed water during immersion in the solution of 3.5% (w/w) NaCl in deionized water, and throughout drying in desiccator almost all the absorbed water in electrocoating film was removed and the film dried completely.

The oscillation amplitude of absorption and excretion of water for sample (N) is more than other samples. According to the results

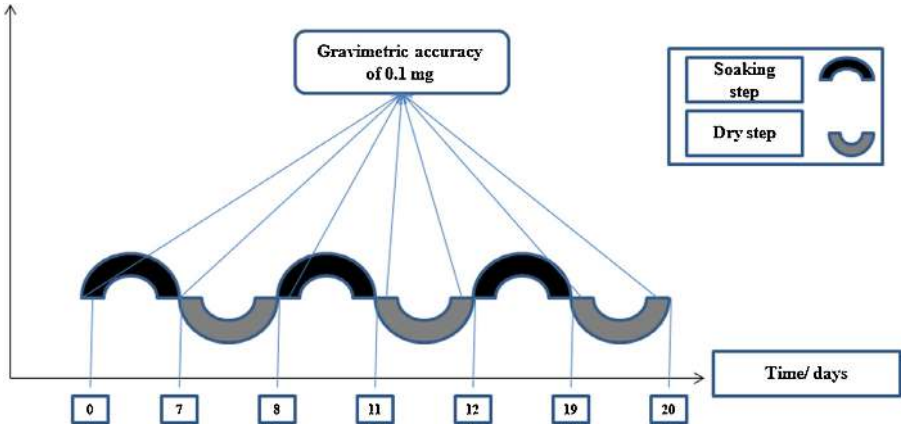

Fig. 3. Time program of gravimetric test during the soaking and dry steps.

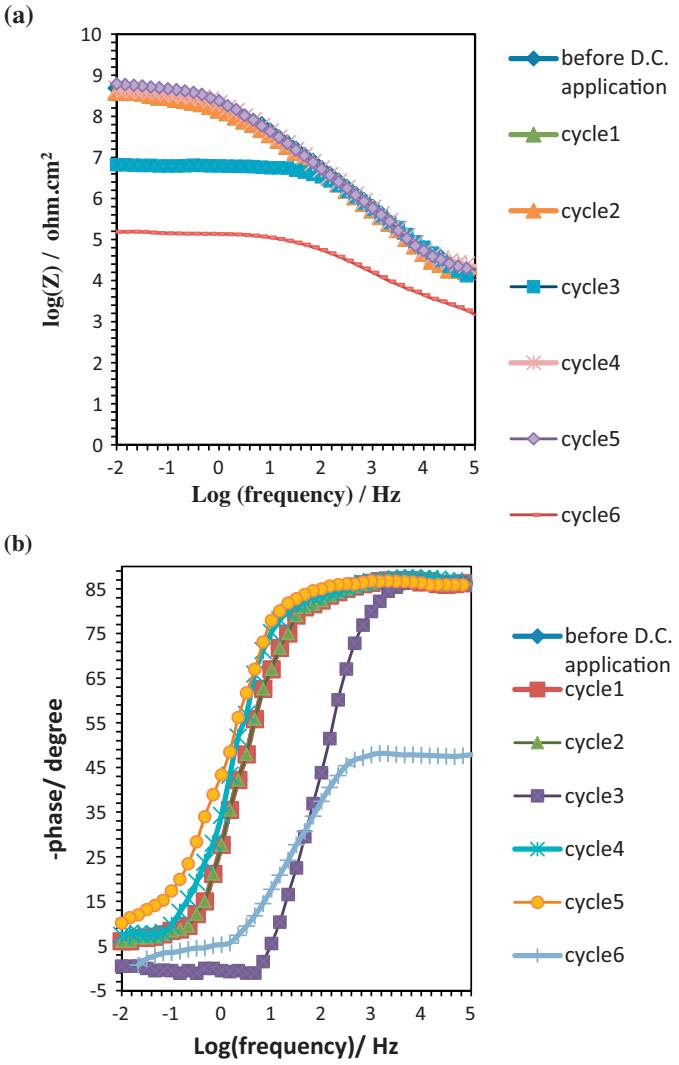

Fig. 4. (a) Bode plots of total impedance of sample (U) at modified AC/DC/AC test. (b) Bode plots of phase angle of sample (U) at modified AC/DC/AC test.

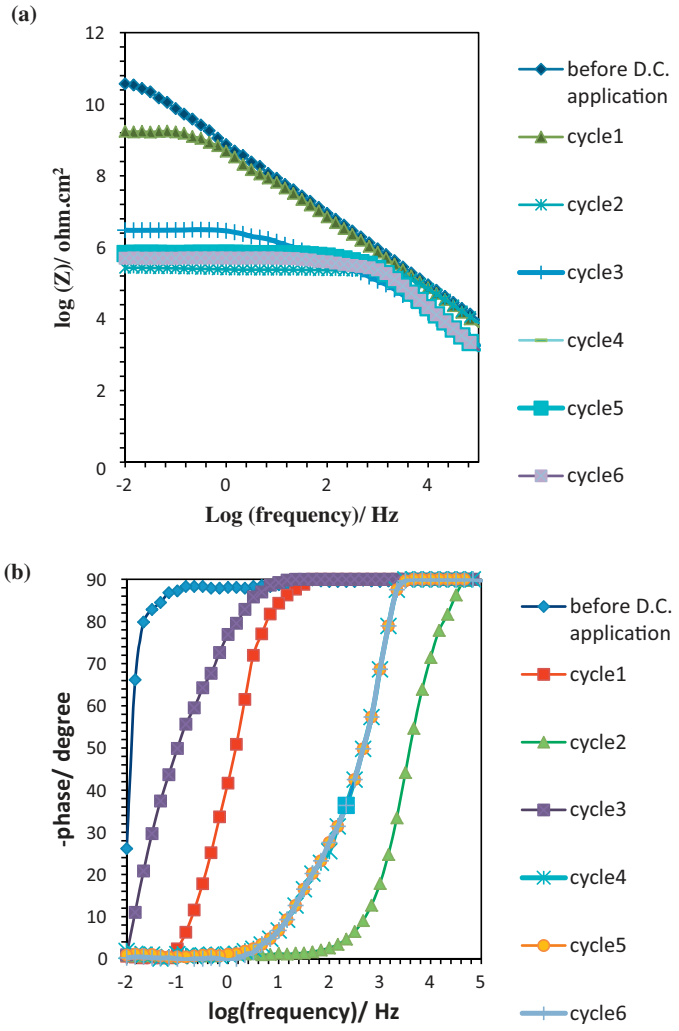

Fig. 5. (a) Bode plots of total impedance of sample (N) at modified AC/DC/AC test. (b) Bode plots of phase angle of sample (N) at modified AC/DC/AC test

of the EIS test in early immersion before DC application, the initial pore resistance of under-baked electrocoating was lower than the other samples. Moreover, according to the results of DSC test, the glass transition temperature of the sample (U) is the lowest one. Because of the high porosity of the sample (U), it can be assumed that the electrocoated film acts as a permeable membrane against the electrolyte absorption and desorption, resulting in simultaneously absorption and desorption of water. On the other side, due to less porosity, the sample N has a balanced absorption and excretion of water during soaking and dry steps, which may be the reason why the remaining water in free volume of normal-baked electrocoating film is the most. Probably because of less pores, it is not possible for the water to completely leave the electrocoated film.

The cyclic water uptake and excretion leads to development of mechanical stresses in the electrocoated films, which finally results in loss of adhesion between the films and the substrates.

The measured weight of the samples confirms the results of modified AC/DC/AC test, therefore, the electrochemical changes in electrocoated samples during the modified AC/DC/AC test are justified.

3.2.2. Mechanical explanation

It was observed that during the DC cycles hydrogen gas was formed at the coating–electrolyte interface. The formed hydrogen gas may result in a large mechanical stress in the coating film. The under-baked sample showed a much higher intensity of gas generation, which is consistent with its low pore resistance. The amount of gas generated at the coating–electrolyte interface increases as the number of wet–DC–dry cycles is raised.

Table 1 shows that the glass transition temperature of the baked films increases by raising the baking temperature. The higher T_g of a thermosetting network is a (direct) result of higher cross-link density and represents a more compact structure. Such a tight network absorbs less water and loses the absorbed water at a slower rate compared to a loose network. So the over-baked coating encounters a lower stress resulting from water uptake. On the other hand, at room temperature the over-baked coating behaves brittle and has a low flexibility (ABS $(T - T_g) = 200$ K), and hence there is a high potential for stress build-up. During the wet and DC cycles, water penetrates into the film and hydrogen gas is formed, respectively. These two phenomena result in a high stress buildup in the over-baked coating, which is the reason for the steep drop of the pore resistance of this sample. The situation is nearly the same for the normal-baked coating. However, the glass transition temperature of the normal-baked coating is not as high as the over-baked coating and in this case the stress buildup would be less.

The under-baked coating has a flexible film that relaxes quickly and the wet–dry cycles do not generate great stresses in the film.

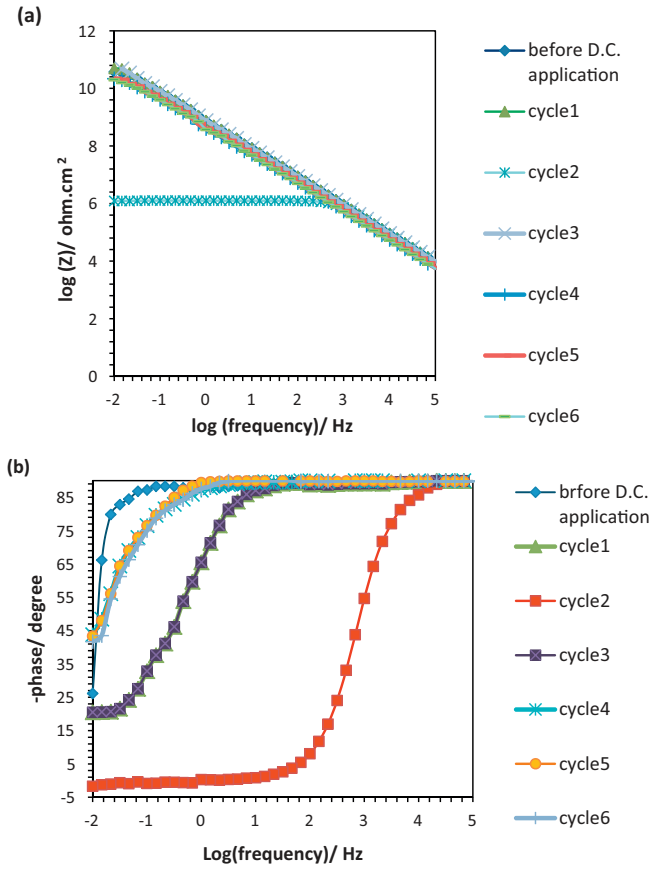

Fig. 6. (a) Bode plots of total impedance of sample (O) at modified AC/DC/AC test. (b) Bode plots of phase angle of sample (O) at modified AC/DC/AC test

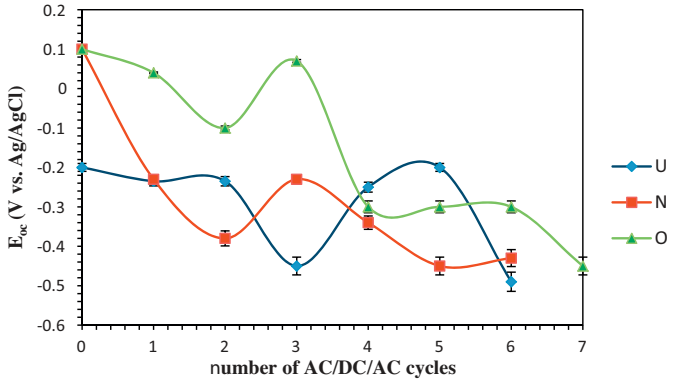

Fig. 7. Stable OCP values of samples at relaxation step after different cycles.

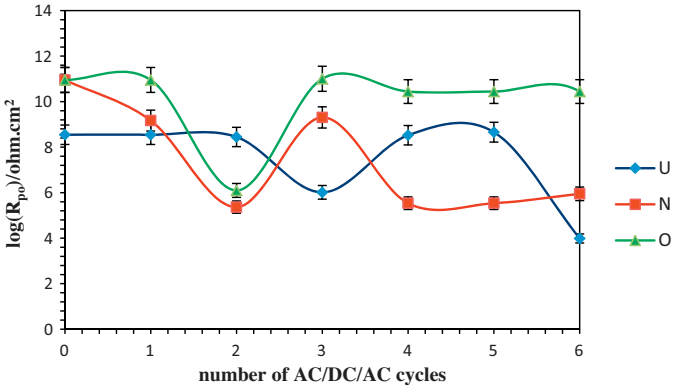

Fig. 8. Pore resistance variations of samples at modified AC/DC/AC test.

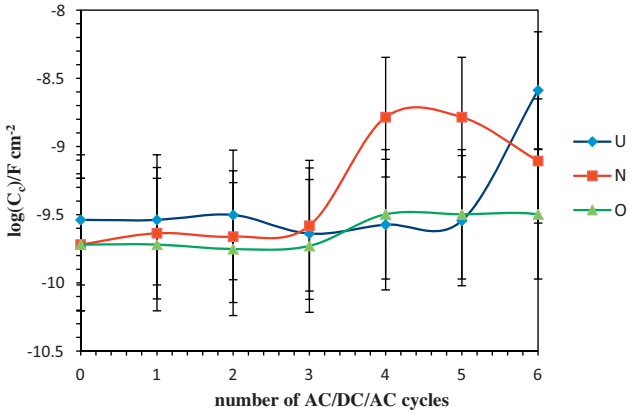

Fig. 9. Coating capacitance variations of samples at modified AC/DC/AC test.

This results in a longer period of time in which the under baked coating maintains its stable OCP value.

3.2.3. *Combined explanation*

The under-baked coating has a loose and flexible network. Thus, due to quick stress relaxation in this coating, the value of initial pore resistance is low and it drops only 2 orders of magnitude upon exposure to consecutive wet–dry cycles.

The over-baked coating has a tight and inflexible network. Hydrogen formation during application of DC potential can generate huge stresses in the film which results in pore formation and a sudden and large drop in the pore resistance of the coating after the critical cycle number. After passing the critical cycle, the corrosion products plug the pores of the coating and get fixed in the film. Therefore the OCP and the pore resistance increase and retain their values.

For the normal baked sample, the film is not as tight as the over-baked sample and is more flexible. So more hydroxyl ions are generated and more pores are formed in this film after the critical cycle. The corrosion products could not be fixed at the coating–metal interface and the pore resistance drops after an initial rise next to the critical cycle.

Light microscopic images of samples are shown in Fig. 11.

As specified in Fig. 11, the sample (N) has the highest pore density and the sample (O) has the lowest pore density. The results of microscopic test of the samples confirm the results of the modified AC/DC/AC test, as the normal-baked electrocoating is less resistant against mechanical stresses, and more pores are formed in its film.

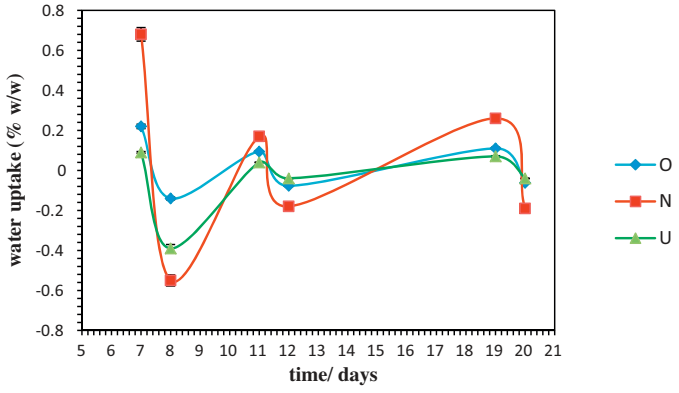

Fig. 10. Absorption and excretion of water during soaking and dry steps of gravimetric test.

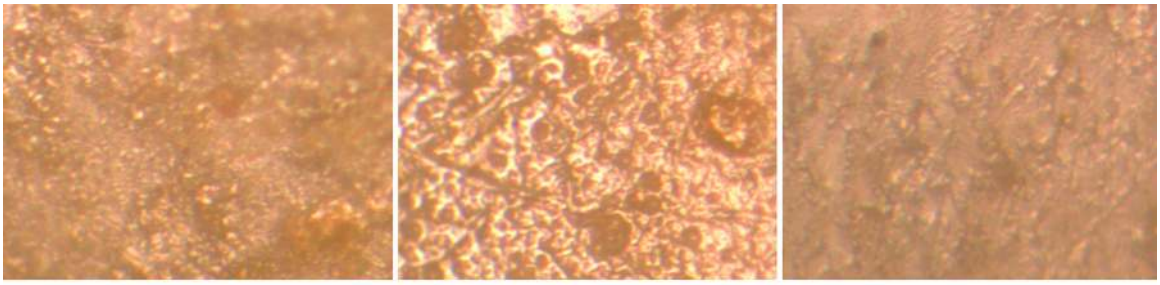

Fig. 11. The images of light microscopic of samples (×400).

Based on the above discussions, a coating which tolerates wet–dry cycles, with a tightly cross-linked film and a high degree of flexibility would be the best choice.

4. Conclusions

The effect of a wet–DC–dry cyclic test on electrochemical characteristics of electrocoats baked at three different conditions was investigated. It was found that the resistive failure is the dominant failure mode of all the coatings in this test. Moreover, the stable OCP and the pore resistance of the coatings are functions of the test cycle and their change with test cycle has the same trend. An electrochemical and a mechanical approach were applied to explain the observed trends. It was found that the coatings with a high flexibility show more stress relaxation properties and therefore maintain their initial properties for a longer period. The coatings which are tightly cross-linked and inflexible are exposed to a great deal of stresses, and sudden changes can be observed in their protective behavior. The more the resistance against mechanical stresses, the later electrochemical failure of the coating during the modified AC/DC/AC test is expected. A combination of high flexibility and tight network would be the ideal choice for a coating which is aimed to tolerate the cyclic corrosion tests.

References

[1] T. Bos, Prediction of Coating Durability, Gildeprintdrukkerijen B.V., Enschede, The Netherlands, 2008.
[2] S.J. Garcia, J. Suay, Prog. Org. Coat. 59 (2007) 251–258.
[3] S.J. Garcia, M.T. Rodriguez, R. Izquierdo b, J. Suay, Prog. Org. Coat. 60 (2007) 303–311.
[4] X. Liu, J. Xiong, Y. Lv, Y. Zuo, Prog. Org. Coat. 64 (2009) 497–503.
[5] W. Walter, Corros. Sci. 26 (1986) 39–47.
[6] J.R. Scully, D.C. Silverman, M.W. Kendig, Electrochemical Impedance: Analysis and Interpretation, ASTM Special Technical Publication, London, 1993.
[7] R. Cottis, S. Turgoose, Electrochemical Impedance and Noise, NACE International, New York, 1999.
[8] D.J. Mills, K. Schaefer, Prog. Org. Coat. 69 (2010) 193–198.
[9] F.D. Wall, M.A. Martinez, N.A. Missert, R.G. Gpeland, A.C. Kilgo, Corros. Sci. 47 (2005) 17–32.
[10] D. Landolt, Corrosion and Surface Chemistry of Metals, CRC Press, New York, 2007.
[11] M. Rashvand, Z. Ranjbar, S. Rastegar, Prog. Org. Coat. 71 (2011) 362–368.
[12] M. Rashvand, Z. Ranjbar, Mater. Corros. 63 (2012) 1–8.
[13] M. Rashvand, Z. Ranjbar, S. Rastegar, J. Electrochem. Soc. 159 (2012) 129–133.
[14] Z. Ranjbar, S. Montazeri, M. Jalili, Prog. Color Colorants Coat. 2 (2009) 23–33.
[15] Q. Zhou, Y. Wang, G.P. Bierwagen, Corros. Sci. 55 (2012) 97–106.
[16] H. Bi, J. Sykes, Corros. Sci. 53 (2011) 3416–3425.
[17] D. Wang, D. Battocchi, K.N. Allahar, S. Balbyshev, G.P. Bierwagen, Corros. Sci. 52 (2010) 441–448.
[18] M.C.S.S. Macedo, I.C.P. Margarit-Mattos, F.L. Fragata, J.-B. Jorcin, N. Pébère, O.R. Mattos, Corros. Sci. 51 (2009) 1322–1327.
[19] J. Hollaender, E. Ludwig, S. Hillebrand, Proceedings of the 5th International Tinplate Conference, London, 1992.
[20] P.A. Sørensena, S. Kiila, K. Dam-Johansen, C.E. Weinell, Prog. Org. Coat. 64 (2009) 142–149.
[21] J. Hollaender, C.A. Schiller, W. Strunz, Proceedings of the EIS 2001, Marilleva, Italy, 2001.
[22] M.T. Rodriguez, J.J. Gracenea, J.J. Saura, J.J. Suay, Prog. Org. Coat. 50 (2004) 123–131.
[23] S.J. Garcia, J.J. Suay, Corros. Sci. 49 (2007) 3256–3275.
[24] M.T. Rodriguez, J.J. Gracenea, J.J. Saura, J.J. Suay, Prog. Org. Coat. 50 (2004) 68–74.
[25] G.P. Bierwagen, K.N. Allahar, Q. Su, V.J. Gelling, Corros. Sci. 51 (2009) 95–101.
[26] N.Q. Su, K. Allahar, G. Bierwagen, Electrochem. Acta 53 (2008) 2825–2830.
[27] K.N. Allahar, G.P. Bierwagen, V.J. Gelling, Corros. Sci. 52 (2010) 1106–1114.
[28] K.N. Allahar, M.E. Orazem, K. Olge, Mathematical model for cathodic delamination using a porosity–pH relationship, Corros. Sci. 49 (2007) 3638–3658.
[29] K.N. Allahar, V. Upadhyay, G.P. Bierwagen, Characterizing the relaxation of the open circuit potential during an AC–DC–AC accelarated test, in: DOD Corrosion Conference, London, 2009.
[30] E.O. Endy, S.F. Cheek, D.C. Stiles, E.W. Corse, Gen. Top. 26 (1992) 2353–2363.
[31] D. Jones, Principle and Prevention of Corrosion, Prentice Hall, Michigan, 1995.
[32] A. Forsgren, Corrosion Control Through Organic Coatings, CRC Press, New York, 2006.
[33] J. Maxted, Corros. Sci. Eng. 2 (1999) (paper 15).
[34] L.F.E. Jacques, Prog. Polym. Sci. 25 (2000) 1337–1362.
[35] B.S. Skerry, C.H. Simpson, Corrosion 49 (1993) 663–674.
[36] A. Nishikata, Y. Ichihara, Y. Mayashi, T. Tsuru, N.D. Tomashov, Corros. Sci. 1 (1961) 77–87.
[37] N.D. Tomashov, Corros. Sci. 4 (1964) 315–334.
[38] J.H. Parke, G.D. Lee, H. Ooshige, A. Nishikata, T. Tsuru, Corros. Sci. 45 (2003) 1881–1894.
[39] R.P. Vera Cruz, A. Nishikata, T. Tsuru, Corros. Sci. 38 (1996) 1397–1406.